Imaging the multi-level magma reservoir at Mt. Etna volcano (Italy)

Marco Aloisi,[1] Mario Mattia,[1] Carmelo Ferlito,[2] Mimmo Palano,[1] Valentina Bruno,[1] and Flavio Cannavò[1]

Received 10 June 2011; revised 15 July 2011; accepted 15 July 2011; published 20 August 2011.

[1] The continuous GPS network operating on Mt. Etna with its 36 stations is currently one of the largest worldwide. The aim of this network is the evaluation of volcanic hazard and the modelling of the active sources. In this paper, we propose an in-depth analysis and modelling of continuous GPS data collected at Mt. Etna from May 2008 to December 2010. The analyzed period has been divided into four different coherent phases: 1) 14 May 2008–02 August 2008 (deflation of the entire GPS network); 2) 02 August 2008–14 June 2009 (deflation of the summit area and inflation at lower heights); 3) 14 June 2009–21 May 2010 (inflation of the entire GPS network); 4) 21 May 2010–31 December 2010 (inflation at medium and low heights and end of the inflation in the summit area). Analytical models indicate a non-uniform deformation style revealing spaced sources acting at different time on different segments of a multi-level magma reservoir. The Etnean plumbing system imaged here is depicted as an elongated magma reservoir that extends from the volcano body downwards to about 6.5 km below sea level (b.s.l.), sloping slightly towards the North-West, with storage volumes located at about 6.5, 2.0 and 0.0 km (b.s.l.). The changes in position of the modelled pressure sources during the analyzed time intervals indicate that, throughout the 2008 eruptive period, the deformation field was mostly driven by the upward migration of magma. On the other hand, the pattern of deformation recorded after the end of the eruption strongly suggests a significant contribution of the magma overpressure generated by the gas boiling, thus outlining the importance of volatiles content in magma. **Citation:** Aloisi, M., M. Mattia, C. Ferlito, M. Palano, V. Bruno, and F. Cannavò (2011), Imaging the multi-level magma reservoir at Mt. Etna volcano (Italy), *Geophys. Res. Lett.*, *38*, L16306, doi:10.1029/2011GL048488.

1. Introduction

[2] Mount Etna volcano (Italy), located along the eastern coast of Sicily (inset in Figure 1), has grown over the last 500 ky due to the accumulation of volcanic products that have risen through a complex plumbing system. The main tectonic axis feeding the volcano is characterized, in its uppermost portion, by an open conduit system that is constantly filled with magma, which undergoes continuous gas exsolution and degassing. Such a feeding regime characterizes the eruptive activity of Mount Etna and the type of emitted products. The amount of degassing is important during eruptive but also non-eruptive periods, as proven by the SO_2 flux, systematically measured by means of COSPEC since 1987 [*Caltabiano et al.*, 2004, and references therein]. The accumulated volume of degassed magma within the plumbing system is huge, considering that about four times more magma degasses than extrudes [e.g., *Ferlito and Lanzafame*, 2010, and references therein], implying that, in the long term, volatiles undergoing degassing come mainly from non-erupted magma. The great amount of magma involved in the persistent activity for centuries has therefore solidified in subvolcanic conditions, constituting the high velocity level detected by seismic tomography [e.g., *Aloisi et al.*, 2002; *Patanè et al.*, 2006]. In this context, a careful analysis of continuously recorded ground deformation data can improve our knowledge about the processes of magma and gas migration in the upper levels of the plumbing system of Mt. Etna. Here, we propose a model where the refilling of the multi-level plumbing system beneath Mt. Etna reveals its complexity and suggests a re-analysis of the interplay between magma and gas in the process of rising from depth.

2. Data and Modelling

[3] The continuous GPS (hereafter, CGPS) monitoring of ground deformations on Mt. Etna started in November 2000. Today, the CGPS network (hereafter, Etn@net) has reached a configuration of 36 stations that cover the volcano edifice entirely (Figure 1). CGPS data collected by the Etn@net network were processed with the GAMIT/GLOBK software packages [*Herring et al.*, 2006] with IGS (International GNNS Service - http://igscb.jpl.nasa.gov) precise ephemerides and Earth orientation parameters from the International Earth Rotation Service (http://www.iers.org), to produce loosely constrained daily solutions, according to the strategy described by *Mattia et al.* [2008]. Through the use of GLOBK software [*Herring et al.*, 2006], the daily solutions were processed in order to estimate the average site velocity in the local "Etn@ref" reference frame [*Palano et al.*, 2010]. Standard error of the GPS solution underestimates the true uncertainty in the GPS velocities [*Zhang et al.*, 1997]. Detailed studies of CGPS data indicate that the noise in GPS time-series may be characterized by a combination of random ('white') and correlated ('colored') noise that depends on several factors, i.e., satellite and tracking network, atmospheric conditions, monument stability, etc. [*Mao et al.*, 1999; *Dixon et al.*, 2000]. In GPS processing with GLOBK, noise is commonly added as a time-dependent random walk error in the velocity estimation. In our case, we added a random walk error of 1 mm/yr$^{1/2}$ which represent an appro-

[1]Osservatorio Etneo, Istituto Nazionale di Geofisica e Vulcanologia, Catania, Italy.
[2]Dipartimento di Geologia, Università degli Studi di Catania, Catania, Italy.

0094-8276/11/2011GL048488

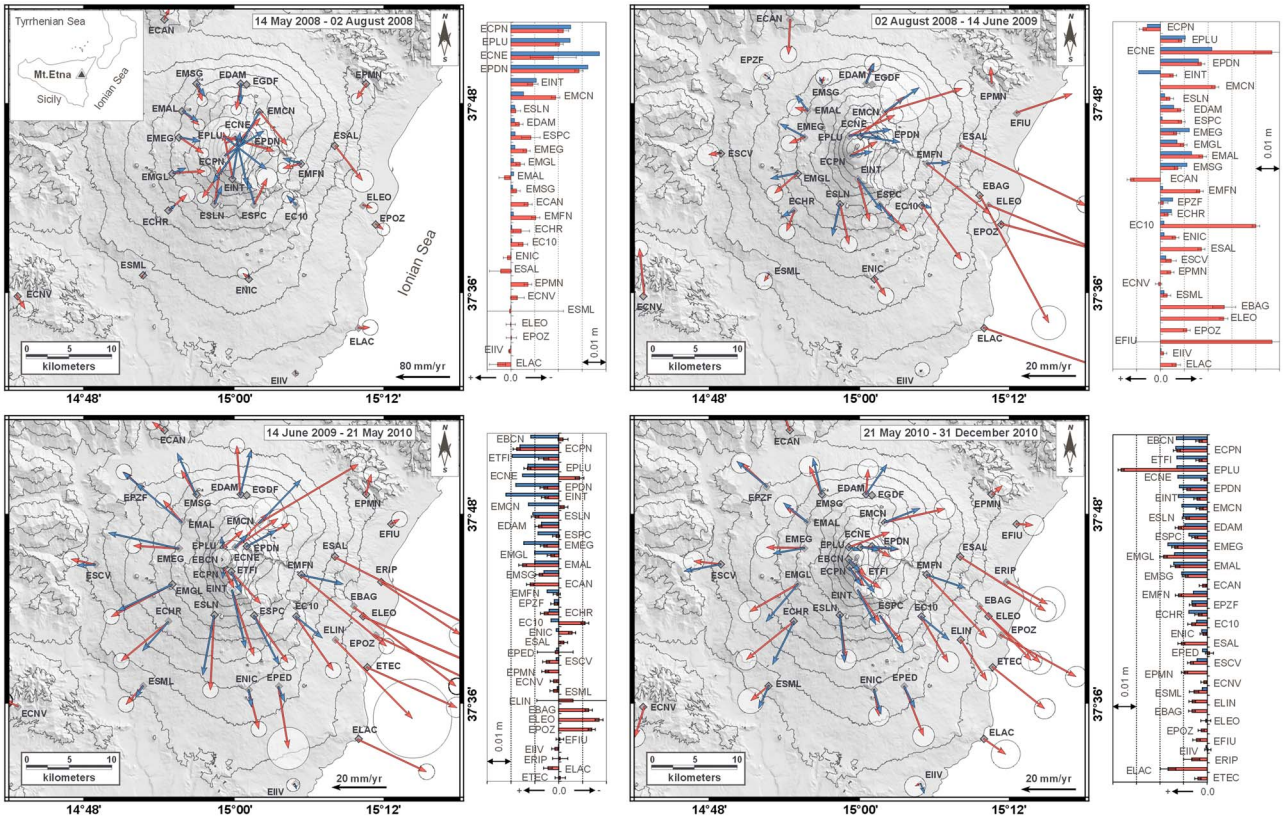

Figure 1. Recorded (red arrows) and modelled (blue arrows) horizontal velocity field for each phase. The histograms report the recorded (red bars) and modelled (blue bars) vertical dislocations for each phase. The vertical variations are sorted by the CGPS station elevations.

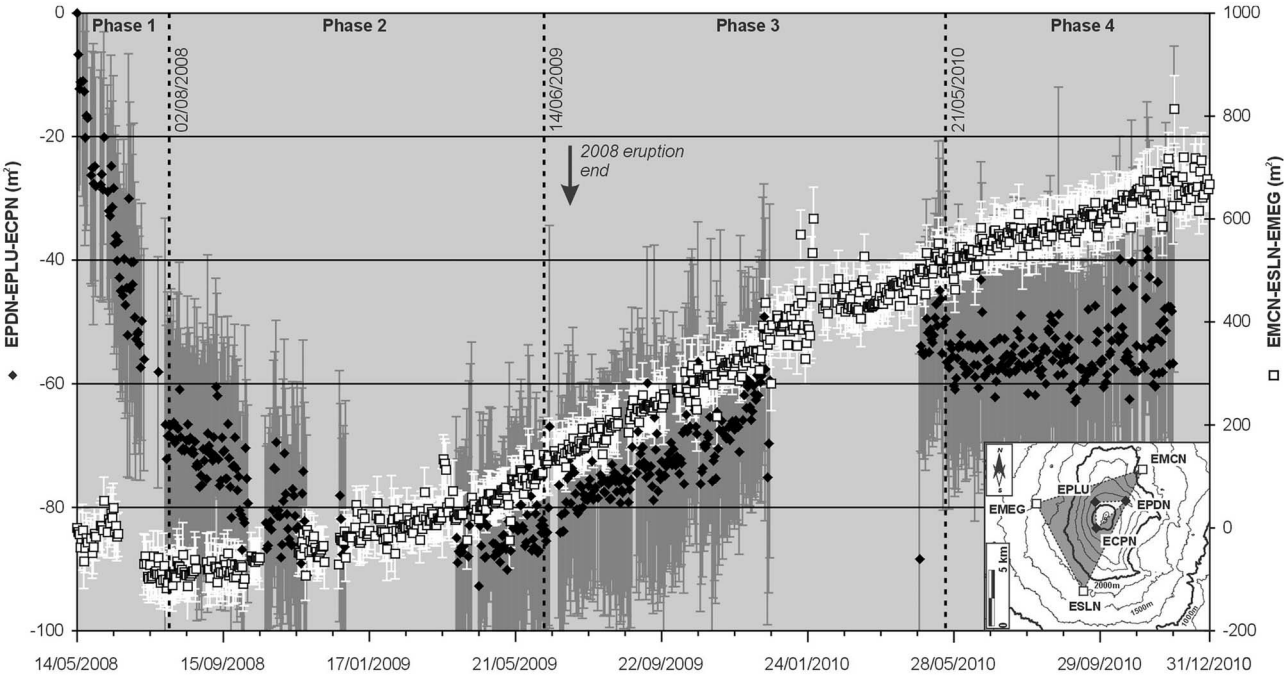

Figure 2. Variation of the area recorded at a summit (EPDN - EPLU - ECPN; black rhombi) and an intermediate altitude triangle (EMCN - ESLN - EMEG; white squares). The error bars are grey for the summit triangle and white for the intermediate triangle. In the inset, the two triangles used to calculate the variation of the area are outlined.

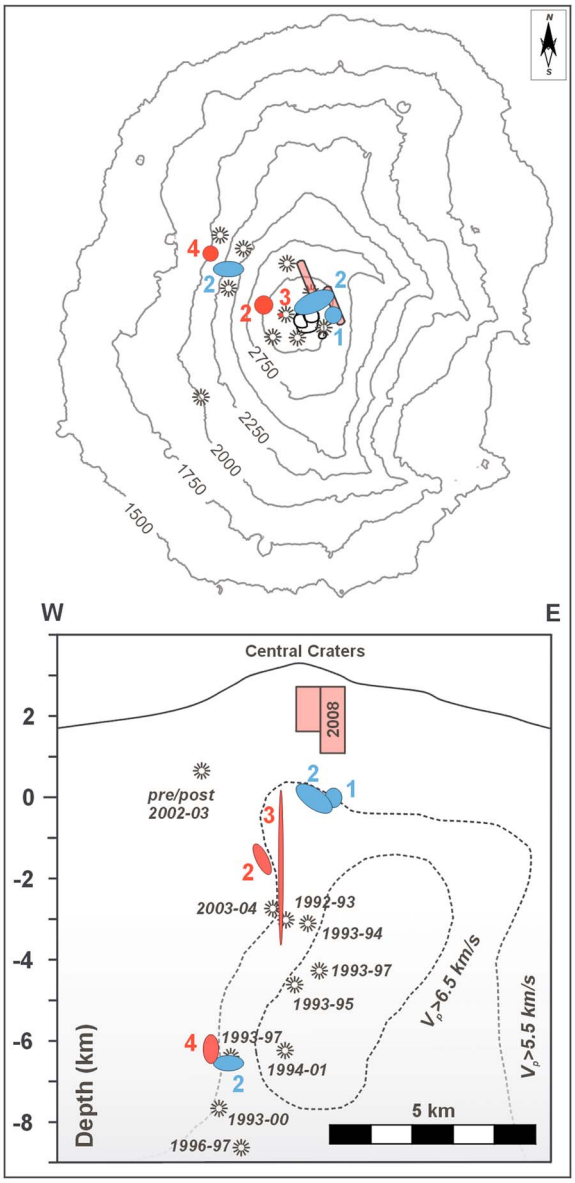

Figure 3. Pressure sources modelled for each phase (inflation in red and deflation in blue). The surface and vertical projection of the modelled 2008 dike-forming intrusions [*Aloisi et al.*, 2009] is shown (light red). The consensus magma pathways (black asterisks) historically resolved by GPS, seismic and other geophysical data are indicated (see *Aloisi et al.* [2011] for an overview). The trace of the high v_p body estimated by *Aloisi et al.* [2002] is also shown. Redrawn by *Aloisi et al.* [2011].

priate error model for Mt. Etna CGPS data [*Palano et al.*, 2010].

[4] We analyzed the CGPS data collected at Mt. Etna from May 2008 to December 2010. The studied period starts after 13 May 2008, when an eruption began accompanied by a strong seismic swarm [e.g., *Aloisi et al.*, 2009]. The 2008 intrusion involved both the SE and the NNE flanks of the volcano, pouring out a volume of magma of about 50 × 10^6 m^3 with an uncertainty of about ±20 percent (D. Andronico, personal communication, 2010). The eruption ended on 7 July 2009. Therefore, the average emission rate was of the order of about 1.5 m^3/s.

[5] For the first time, the spatial density reached by the CGPS network enabled a detailed analysis of the geophysical processes acting at different spatial and temporal scales. In particular, the variation of area calculated for two triangles (Figure 2), one related to three summit GPS stations (EPDN-EPLU-ECPN) and the other related to three intermediate altitude GPS stations (EMCN-ESLN-EMEG), showed a different behaviour, allowing us to separate the analyzed period into four different phases. During the first phase (14 May 2008–02 August 2008), both the triangles showed a similar trend related to an overall deflation following the beginning of the 2008 eruption. The second phase (02 August 2008–14 June 2009), showed a more complex deformation pattern with a deflation of the summit area and an inflation at lower heights. The third phase (14 June 2009–21 May 2010), following the end of the 2008 eruption, was characterized by an inflation over the entire scale of the CGPS network. Finally, the fourth phase (21 May 2010–31 December 2010), showed an inflation at medium height without significant areal changes at the summit triangle.

[6] We modelled the recorded deformation pattern as induced by pressure sources acting inside the volcano. We used the entire CGPS network except the stations ECAN, ECNV and EPMN (Figure 1) which are located far outside the volcano edifice. Moreover, the eastern flank of the volcano is affected by an almost constant ESE-ward motion whose origin is still controversial and is most likely not directly linked to the dike-like intrusions (for a review see, e.g., *Aloisi et al.* [2011]). Therefore, for this modelling aimed at imaging the volcano plumbing system, we did not take into account the GPS stations located on the eastern flank of the volcano (EFIU, ELAC, ELEO, ELIN, EPOZ, ERIP, ESAL and ETEC; Figure 1). We performed an analytical inversion of CGPS data, describing the pressure source with the arbitrarily oriented, finite, prolate and spheroidal cavity embedded in an elastic half-space of *Yang et al.* [1988]. We chose this source model among the other models published in literature [e.g., *Mogi*, 1958; *Davis*, 1986; *McTigue*, 1987], since it shows a good trade-off in this case between the number of degrees of freedom and the obtained data fit. In particular, *Mogi*'s [1958] source is too simple to explain the complex and non-uniform recorded deformation pattern. On the contrary, *Davis*' [1986] source doesn't improve the fit significantly, despite having one more parameter than *Yang et al.*'s [1988] source. Moreover, the finite model is more accurate in the near field with respect to the point model [*Yang et al.*, 1988]. The pressure source is determined by eight parameters: the coordinates x_c and y_c of the spheroid centre, the coordinate z_c of the spheroid centre depth, the azimuth θ measured counterclockwise from the positive y direction around the z axis, the dipping angle φ measured clockwise from the positive y direction around the x axis, the major semi-axis a, the ratio b/a between the minor and major axes, the intensity of the pressure P on the surface of the spheroid. It is well known that there is a trade-off between the crustal strength, the source pressure and the related volume [e.g., *Davis*, 1986; *Yang et al.*, 1988; *Newman et al.*, 2006]. Hence, we might obtain a large uncertainty on the estimation of source pressure if we do not know the rheology

Table 1. Model Parameters and Related Uncertainties[a]

Parameters	Phase 1 Source 1	Phase 2			Phase 3 Source 1	Phase 4 Source 1
		Source 1	Source 2	Source 3		
x_c [m]	500472 ± 136	499972 ± 248	498464 ± 291	497409 ± 159	498964 ± 982	496909 ± 698
y_c [m]	4178447 ± 137	4178946 ± 59	4178756 ± 101	4179767 ± 198	4178413 ± 581	4180267 ± 596
z_c [m]	0 ± 158	−20 ± 123	−1585 ± 127	−6609 ± 261	−1805 ± 2005	−6109 ± 1957
θ [°]	119.4 ± 53.5	114.3 ± 81.2	89.2 ± 55.4	98.8 ± 75.5	180.0 ± 60.6	180.0 ± 76.4
φ [°]	164.9 ± 76.4	144.4 ± 82.6	116.3 ± 16.3	0.0 ± 82.8	85.3 ± 9.7	78.2 ± 21.0
a [m]	243 ± 75	522 ± 143	416 ± 447	374 ± 455	1913 ± 454	357 ± 397
b/a	0.860 ± 0.149	0.302 ± 0.302	0.350 ± 0.272	0.513 ± 0.291	0.030 ± 0.244	0.529 ± 0.249
P [Pa]	−1.5E + 09 ± 2.9E + 09	−1.4E + 09 ± 3.1E + 09	8.3E + 09 ± 3.0E + 09	−6.4E + 09 ± 3.2E + 09	6.7E + 09 ± 2.7E + 09	6.0E + 09 ± 2.7E + 09
ΔV [m^3]	*−1.0E + 07*	*−1.2E + 07*	*4.6E + 07*	*−5.5E + 07*	*2.7E + 07*	*4.8E + 07*

[a]ΔV is calculated according to *Tiampo et al.* [2000] using a value of the effective shear modulus μ equal to 5 GPa.

and source volume. In practice, this means that in order to estimate reasonable source pressures we must assume plausible source volumes and a correct rheology. The first phase lasted 81 days and taking into account that the average emission rate was of the order of about 1.5 m^3/s (D. Andronico, personal communication, 2010), a magma volume of about 10×10^6 m^3 was poured out. Therefore, using a suitable rigidity value μ for hot volcanic region of 5 GPa [e.g., *Bonafede et al.*, 1986; *Davis*, 1986; *Bonaccorso et al.*, 2005; *Newman et al.*, 2006], we chose to limit the source volume change for the first phase to a maximum value of 10×10^6 m^3, as estimated during the 2008 eruption. Moreover, during the later three stages we left the intensity of the pressure P free to vary at most by one order of magnitude around the absolute value of P obtained for the first phase.

[7] The inversion was performed by using the Genetic Algorithms (GA) approach, a well-known and robust bio-inspired search technique widely used in computing to solve non-linear optimization problems and categorized as global heuristics search [*Goldberg*, 1989]. Successively, starting from the optimum solutions obtained for each of the four phases by using the GA approach, we applied the pattern search technique which performs a search on a dynamic grid over the space of the source parameters [*Lewis and Torczon*, 1999]. Finally, to estimate the uncertainty of each optimal source parameter, a Jackknife re-sampling method [*Efron*, 1982] was adopted. We included the effects of the topography using the varying-depth model of *Williams and Wadge* [1998] that assumes a different elevation for each recording station corresponding to the actual elevation of the point.

[8] Final optimal solutions for each phase are shown in Figure 3 and Table 1. The modelled and recorded deformation pattern is shown in Figure 1. We obtained a reduced chi-squared equal to 1.0 considering the horizontal and vertical displacements with an a-posteriori standard deviation of 0.005 and 0.008, 0.010 and 0.017, 0.007 and 0.011, 0.003 and 0.009 meters, for the four phases respectively. During the first phase, the obtained pressure source perfectly coincides in position with the dike-like intrusion that was modelled for the 2008 eruption onset [*Aloisi et al.*, 2009]. In this framework, this almost spherical pressure source located near the base of the modelled dike-like intrusion, at the sea level, could represent the magma storage that fed the 2008 eruption, producing a deflation at the entire scale of the CGPS network (Figure 3). Even if the shallow depressurization source also remains active during the second phase (Figure 3), until the end of the eruption, it is not fully able to explain the deflation of the summit area, the inflation recorded at lower heights (Figure 2) and the lowering in elevation simultaneously recorded by the entire CGPS network (Figure 1). We verified that this complex deformation pattern can be explained by adding two other pressure sources to the shallow deflation source. These two sources are compatible in position with the optimal solutions that we found for the following two phases. Therefore, to have an homogeneous solution for the overall analyzed period, we used as starting models for the second phase the optimal solutions obtained respectively for the first, third and fourth phases, limiting the ranges of variability for the parameters x_c, y_c and z_c to ±500 m, which is the arithmetic mean of the calculated uncertainties for the same parameters (Table 1). As for the first period, the shallow pressure source continued to feed the 2008 eruption but it becomes a little more elongated than a spherical shape (Figure 3 and Table 1). Moreover, we obtained a deflating source at a depth of about 6.6 km (b.s.l.) together with an inflating source located at an intermediate depth of about 1.5 km (b.s.l). We determine that a batch of magma ascended toward the zone of neutral buoyancy corresponding with the position where we found the intermediate source. During the third phase, the intermediate source of inflation is still active (Figure 3) and the obtained better solution was an elongated pressure cavity, ranging from about 4 km to 0 km (b.s.l.). Finally, during the last phase, the deformation pattern was explained by a deep pressure source of inflation located at about 6.1 km (b.s.l.) and characterized by a spheroidal shape vertically elongated.

3. Discussion and Conclusions

[9] The high quality of data collected on the current dense configuration of the Etn@net CGPS network permits a detailed analysis of the mechanisms of magma migration from depth and, therefore, allows a fast and accurate evaluation of volcanic hazard. In particular, the analysis proposed here highlights two significant characteristics: 1) during a generally non-homogeneous phase (either deflation and inflation recorded at different altitudes at the same time) it is possible to envisage different sources contemporaneously acting beneath the volcano; 2) the inflation sources undergo a progressive deepening in time, as displayed in phases three and four (Figure 3). The co-existence of different sources acting contemporaneously, imaged here for the first time, is very likely related to the enhanced resolution ability of the CGPS network.

[10] We determine that, throughout the 2008 eruptive period, the recorded deformation pattern (Figure 1) is compatible with a batch of magma rising from about 6.5 km (b.s.l.) toward the zone of neutral buoyancy corresponding with the position where we found the intermediate source (about 2 km b.s.l.). In turn, the intermediate source feeds the shallow source, simultaneously feeding the 2008 eruption (Figure 3).

[11] The explanation of the progressive deepening in time of the inflation sources is not a simple problem. Indeed, if we hypothesize that the inflation is caused by a batch of magma progressively rising toward the surface, the temporal displacement of the pressure source should have the opposite polarity, moving from deep to shallow levels. Therefore, the progressive deepening of the pressure source observed in phases three and four must be explained by another way. We suggest that the observed pattern is consistent with the overpressure provided to the magma by the gas exsolution and boiling. Volatiles dissolved in magma can exsolve and boil when solubility is reached. This depends, for each volatile species, on the relative concentration in magma, pressure and temperature. The latter parameter does not vary significantly in natural magmas, whereas pressure and concentration can display significant variations. In particular, pressure will constantly decrease as magma rises to the surface, promoting gas boiling and ultimately the eruption. Gas boiling also can be caused by a relative increase of the content of volatiles in residual magma during crystal fractionation process occurring within the magma chamber and/or magma conduits or by the fluid migration irrespective of magma. The likelihood of this process, invoked to explain the increment of alkali in relatively shallow residing magmas [*Ferlito et al.*, 2009; *Ferlito and Lanzafame*, 2010], may be confirmed by the almost constant content of SO_2 in Mt. Etna's plume [*Caltabiano et al.*, 2004]. The large quantities of volatiles passing through magmas in the plumbing system can reach saturation and bring about magma overpressure in accordance with the deformation pattern observed in phases three and four. In fact, the magma located in the higher portion of the plumbing system and subjected to lower confining pressure, reaches saturation first whereas the deeper residing magma subjected to higher confining pressure needs more time to reach saturation and generate the overpressure necessary to trigger inflation.

[12] In this framework, the deformation field recorded throughout the 2008 eruptive period was mostly driven by the upward migration of magma whereas, after the end of the eruption, the deformation pattern was mainly due to the magma overpressure generated by the gas boiling. Moreover, the location of the detected pressure sources, acting during the four phases, confirms that the plumbing system of Mt. Etna is elongated in the western sector as found by tomographic analysis [e.g., *Aloisi et al.*, 2002; *Patanè et al.*, 2006] (Figure 3) and by the attenuation tomography [*De Gori et al.*, 2005].

[13] If the pattern of source deepening observed during the studied period is confirmed by the analyses of future deformation, the role of the volatiles in triggering deformation could be considered as significant and therefore relevant for monitoring purposes. Indeed, the observation of future progressive deepening in time of the inflating source revealed by the CGPS data could indicate a greater likelihood of an eventual next eruption characterized by more explosive activity.

[14] **Acknowledgments.** We thank Daniele Pellegrino and Mario Pulvirenti for their fundamental contributions in the installation and maintenance of the CGPS network at Mt. Etna and for their dedication and enthusiasm. We also thank Massimo Rossi for his fundamental work of data processing and automation of several analysis procedures. Finally, we thank Michael Lisowski and an anonymous reviewer for their useful reviews and for their appreciation of the high quality of the CGPS time series here discussed.

[15] The Editor thanks Mike Lisowski and an anonymous reviewer for their assistance in evaluating this paper.

References

Aloisi, M., O. Cocina, G. Neri, B. Orecchio, and E. Privitera (2002), Seismic tomography of the crust underneath the Etna volcano, Sicily, *Phys. Earth Planet. Inter.*, *134*, 139–155, doi:10.1016/S0031-9201(02)00153-X.

Aloisi, M., A. Bonaccorso, F. Cannavò, S. Gambino, M. Mattia, G. Puglisi, and E. Boschi (2009), A new dike intrusion style for the Mount Etna May 2008 eruption modelled through continuous tilt and GPS data, *Terra Nova*, *21*, 316–321, doi:10.1111/j.1365-3121.2009.00889.x.

Aloisi, M., M. Mattia, C. Monaco, and F. Pulvirenti (2011), Magma, faults, and gravitational loading at Mount Etna: The 2002–2003 eruptive period, *J. Geophys. Res.*, *116*, B05203, doi:10.1029/2010JB007909.

Bonaccorso, A., S. Cianetti, C. Giunchi, E. Trasatti, M. Bonafede, and E. Boschi (2005), Analytical and 3D numerical modeling of Mt. Etna (Italy) volcano inflation, *Geophys. J. Int.*, *163*(2), 852–862, doi:10.1111/j.1365-246X.2005.02777.x.

Bonafede, M., M. Dragoni, and F. Quareni (1986), Displacement and stress fields produced by a centre of dilation and by a pressure source in a viscoelastic half-space: Application to the study of ground deformation and seismic activity at Campi Flegrei, Italy, *Geophys. J. R. Astron. Soc.*, *87*, 455–485.

Caltabiano, T., M. Burton, S. Giammanco, P. Allard, N. Bruno, F. Murè, and R. Romano (2004), Volcanic gas emissions from the summit craters and flanks of Mt. Etna, 1987–2000, in *Mt. Etna: Volcano Laboratory*, *Geophys. Monogr. Ser.*, vol. 143, edited by A. Bonaccorso et al., pp. 111–128, AGU, Washington, D. C.

Davis, P. M. (1986), Surface deformation due to inflation of an arbitrarily oriented triaxial ellipsoidal cavity in an elastic half-space, with reference to Kilauea volcano, Hawaii, *J. Geophys. Res.*, *91*, 7429–7438, doi:10.1029/JB091iB07p07429.

De Gori, P., C. Chiarabba, and D. Patanè (2005), Qp structure of Mount Etna: Constraints for the physics of the plumbing system, *J. Geophys. Res.*, *110*, B05303, doi:10.1029/2003JB002875.

Dixon, T. H., M. M. Miller, F. Farina, H. Wang, and D. Johnson (2000), Present-day motion of the Sierra Nevada block and some tectonic implications for the Basin and Range province: North American Cordillera, *Tectonics*, *19*, 1–24, doi:10.1029/1998TC001088.

Efron, B. (1982), *The Jackknife, Bootstrap and Other Resampling Plans*, Soc. for Ind. and Appl. Math., Philadelphia, Pa.

Ferlito, C., M. Viccaro, and R. Cristofolini (2009), Volatile-rich magma injection into the feeding system during the 2001 eruption of Mt. Etna (Italy): Its role on explosive activity and change in rheology of lavas, *Bull. Volcanol.*, *71*, 1149–1158, doi:10.1007/s00445-009-0290-x.

Ferlito, C., and G. Lanzafame (2010), The role of supercritical fluids in the potassium enrichment of magmas at Mount Etna volcano (Italy), *Lithos*, *119*, 642–650, doi:10.1016/j.lithos.2010.08.006.

Goldberg, D. E. (1989), *Genetic Algorithms in Search, Optimization and Machine Learning*, Kluwer Acad., Boston, Mass.

Herring, T. A., R. W. King, and S. C. McKlusky (2006), *Introduction to GAMIT/GLOBK Release 10.3*, Mass. Inst. of Technol., Cambridge.

Lewis, R. M., and V. Torczon (1999), Pattern search algorithms for bound constrained minimization, *SIAM J. Optim.*, *9*(4), 1082–1099, doi:10.1137/S1052623496300507.

Mao, A., C. G. A. Harrison, and T. H. Dixon (1999), Noise in GPS coordinate time series, *J. Geophys. Res.*, *104*, 2797–2816, doi:10.1029/1998JB900033.

Mattia, M., M. Palano, V. Bruno, F. Cannavò, A. Bonaccorso, and S. Gresta (2008), Tectonic features of the Lipari–Vulcano complex (Aeolian archipelago, Italy) from 10 years (1996–2006) of GPS data, *Terra Nova*, *20*, 370–377, doi:10.1111/j.1365-3121.2008.00830.x.

McTigue, D. F. (1987), Elastic stress and deformation near a finite sphericalmagma body: Resolution of the point source paradox, *J. Geophys. Res.*, *92*, 12,931–12,940, doi:10.1029/JB092iB12p12931.

Mogi, K. (1958), Relations between the eruptions of various volcanoes and the deformations of the ground surface around them, *Bull. Earthquake Res. Inst. Univ. Tokyo*, *36*, 99–134.

Newman, A. V., T. H. Dixon, and N. Gourmelen (2006), A four-dimensional viscoelastic deformation model for Long Valley Caldera, California, between 1995–2000, *J. Volcanol. Geotherm. Res.*, *150*, 244–269, doi:10.1016/j.jvolgeores.2005.07.017.

Palano, M., M. Rossi, F. Cannavò, V. Bruno, M. Aloisi, D. Pellegrino, M. Pulvirenti, G. Siligato, and M. Mattia (2010), Etn@ref: A geodetic reference frame for Mt. Etna GPS networks, *Ann. Geophys.*, *53*, 49–57, doi:10.4401/ag-4879.

Patanè, D., G. Barberi, O. Cocina, P. De Gori, and C. Chiarabba (2006), Time-resolved seismic tomography detects magma intrusions at Mount Etna, *Science*, *313*, 821–823, doi:10.1126/science.1127724.

Tiampo, K. F., J. B. Rundle, J. Fernandez, and J. O. Langbein (2000), Spherical and ellipsoidal volcanic sources at Long Valley Caldera, California, using a genetic algorithm inversion technique, *J. Volcanol. Geotherm. Res.*, *102*, 189–206, doi:10.1016/S0377-0273(00)00185-2.

Williams, C. A., and G. Wadge (1998), The effects of topography on magma chamber deformation models: Application to Mt. Etna and radar interferometry, *Geophys. Res. Lett.*, *25*, 1549–1552, doi:10.1029/98GL01136.

Yang, X. M., P. M. Davis, and J. H. Dieterich (1988), Deformation from inflation of a dipping finite prolate spheroid in an elastic half-space as a model for volcanic stressing, *J. Geophys. Res.*, *93*, 4249–4257, doi:10.1029/JB093iB05p04249.

Zhang, J., Y. Bock, H. Johnson, P. Fang, J. F. Genrich, S. Williams, S. Wdowinski, and J. Behr (1997), Southern California Permanent GPS Geodetic Array: Error analysis of daily position estimates and site velocities, *J. Geophys. Res.*, *102*, 18,035–18,055, doi:10.1029/97JB01380.

M. Aloisi, V. Bruno, F. Cannavò, M. Mattia, and M. Palano, Osservatorio Etneo, Istituto Nazionale di Geofisica e Vulcanologia, Piazza Roma 2, I-95123 Catania, Italy. (marco.aloisi@ct.ingv.it)

C. Ferlito, Dipartimento di Geologia, Università degli Studi di Catania, Corso Italia, 57, I-95129 Catania, Italy.